Ocean Sci. Discuss., 10, 727–762, 2013
www.ocean-sci-discuss.net/10/727/2013/
doi:10.5194/osd-10-727-2013

Ocean Science Discussions
Open Access

Discussion Paper | Discussion Paper | Discussion Paper | Discussion Paper |

Estuarine circulation reversals and related rapid changes in winter near-bottom oxygen conditions in the Gulf of Finland, Baltic Sea

T. Liblik, J. Laanemets, U. Raudsepp, J. Elken, and I. Suhhova

Marine Systems Institute, Tallinn University of Technology, Akadeemia Road 15a, 12618 Tallinn, Estonia

Received: 25 March 2013 – Accepted: 28 March 2013 – Published: 12 April 2013

Correspondence to: T. Liblik (taavi.liblik@msi.ttu.ee)

Published by Copernicus Publications on behalf of the European Geosciences Union.

Abstract

The reversal of estuarine circulation caused by southwesterly wind forcing may lead to vanishing of stratification and oxygenation of deep layers during the cold season in the Gulf of Finland. Six CTD+oxygen transects (130 km long, 10 stations) were conducted along the thalweg from the western border to the central gulf (21 December 2011–8 May 2012). Two bottom-mounted ADCP, near the western border and in the central gulf were installed. A CTD with dissolved oxygen sensor was deployed close to the western ADCP. Periods with typical estuarine circulation were characterized by strong stratification; high salinity, hypoxic conditions and inflow to the gulf in the near bottom layer. Two circulation reversals were observed, in December–January and February–March. The first well-developed reversal event caused the vanishing of stratification and oxygen concentrations that were almost over 270 µmol L^{-1} (6 mL L^{-1}) in the entire water column along the transect; and lasted for about 1.5 months. Shifts from estuarine circulation to reversed circulation and vice versa were both associated with strong currents (up to 40 cm s^{-1}) in the deep layer. In the western area of study, near-bottom oxygen conditions strongly depended on salt wedge intrusions (hypoxic water) from the NE Baltic Proper, while in the eastern part good oxygen conditions caused by reversals remained for a few months. Change from oxygenated to hypoxic conditions in the entrance area to the Gulf might occur very rapidly, within less than a day.

1 Introduction

The bottom of the Baltic Sea is the largest dead zone in the world (Diaz and Rosenberg, 2008). Hypoxia (oxygen concentration of less than 90 µmol L^{-1} or 2 mL L^{-1}) has been present during the last 8000 yr in the Baltic Sea (Zillén et al., 2008). Nevertheless, the present extent of hypoxia in the Baltic Sea can be partly connected to the anthropogenic nutrient load and concurrent eutrophication (Conley et al., 2009). Eutrophication leads to increased sedimentation of organic material, thus increasing the

OSD
10, 727–762, 2013

area of anoxic bottoms and internal phosphorus loading. In addition, the hypoxic water volume displays a negative correlation with the total dissolved inorganic nitrogen pool, i.e. greater overall nitrogen removal with increased hypoxia (Vahtera et al., 2007). Hypoxia-related effects to the benthic ecosystem (e.g. Laine et al., 2007) and biogeochemical cycles of nutrients (e.g. Jäntti and Hietanen, 2012) are evident in the Gulf of Finland.

During 1961–2005, the hypoxic zone extended on average over an area of about 50 000 km^2 in the Baltic Sea (Savchuk, 2010). Deep layers of the Baltic Proper are supplied with oxygen only during major inflows from the North Sea by lateral advection. However, such inflows also strengthen the stratification due to the higher salinity of "new water." It has been demonstrated that intermediate depths of the water column (80–120 m) had higher oxygen concentrations during the so-called stagnation period in the Baltic Sea (Conley et al., 2002). The last remarkable ventilation of the Baltic Proper deep layers was observed after the major inflow in 1993 (Matthäus and Lass, 1995), when oxygen concentration in the Gotland deep rose to 2 mL L^{-1}; however, oxygen again disappeared in 1998 (Fonselius and Valderrama, 2003).

Since the deep water of the Gulf of Finland originates near the halocline of the Baltic Proper, the strong and shallow halocline in the Baltic Proper induces stronger stratification and hypoxia in the Gulf of Finland. The relatively weaker and deeper halocline in the Baltic Proper induces weaker stratification and reduction of the hypoxia in the Gulf of Finland (Conley et al., 2009). It has been shown that the halocline was stronger (Liblik and Lips, 2011) and oxygen depletion increased (Laine et al., 2007) in the Gulf of Finland after the major inflow of North Sea waters in 1993.

Elken et al. (2003) showed on the basis of summer CTD measurements that the halocline disappearance could occur when the southwesterly (nearly up-estuary) wind forcing caused the reversal of estuarine circulation in the gulf: the surface layer flows into the estuary and the deep layer flows out, in opposition to normal estuarine circulation. On the contrary, northeasterly and northerly winds support standard estuarine circulation, resulting in stronger stratification (Elken et al., 2003; Liblik and Lips, 2011) and importation of phosphorus-rich waters from the deeper sub-halocline layers of the Baltic Proper (Lips et al., 2008). Elken et al. (2012) analyzed routine CTD measurements and wind data over several decades to investigate possible changes in the frequency of wintertime stratification collapse events. They found that the bottom-to-surface density difference becomes close to zero (note that wintertime is already characterized by the weakest stratification in the Gulf, see Haapala and Alenius, 1994) during wind-induced strong estuarine circulation reversal events caused by up-estuary (southwesterly) wind forcing. They also found that since the 1990s the frequency and duration of such stratification collapse events have increased due to the shift in wind regime, i.e. the considerable increase of westerly-southwesterly wind impulse in December–January. It is commonly understood that mixing of the entire water column will improve the near-bottom oxygen conditions either (1) by direct vertical stirring processes only, or (2) by stirring in combination with wind-induced straining (differential lateral advection), with the latter factor dominating. These two types of mixing could supposedly have different change rates of near-bottom salinity and oxygen (resulting perhaps also in different release rates of phosphorus from the sediments), but these rates of change remained formerly unknown because of missing purpose-oriented observations.

The main aim of the present study was to observe and map details of winter stratification changes in the Gulf of Finland (as a model for the large non-tidal estuary), in order to identify under what conditions the stratification collapse events occur: whether they are caused primarily by estuarine circulation reversals, or if the vertical stirring dominates; and to estimate the effect of these events on the spatio-temporal variability of oxygen concentration in the deep layer of the gulf. When planning the studies, we supposed as a hypothesis that reversal of the estuarine circulation and concurrent disappearance of the salt wedge could rapidly and remarkably alter oxygen conditions in the deep layer of the Gulf of Finland.

Following the description of the study area and the methods used, the presentation is based on the analysis of (1) regular time series of wind conditions, (2) repeated

OSD
10, 727–762, 2013

transects of CTD and O_2 along the thalweg, and (3) time series observations at two deep mooring locations: ADCP recording of current profiles and near-bottom point-recording of CTD and O_2 The presentation and analysis of observational results is followed by discussion and conclusions.

2 Study area, data and methods

2.1 Study area and surveys

The Gulf of Finland lies in the northeastern part of the Baltic Sea (Fig. 1). Due to the relative isolation of the Baltic Sea from the ocean, tidal oscillations of the sea level are of minor importance to the dynamics of the gulf (e.g. Kullenberg, 1981), which is quite unique among the world's estuaries (Hansen and Rattray, 1966; MacCready and Geyer, 2010). The length of the gulf is about 400 km and its width varies from 48 to 135 km; maximum depths exceed 100 m in the central and western areas. River discharge is concentrated in the eastern part of the gulf, where the Neva River inflow is on average 77.6 $km^3 yr^{-1}$, i.e. about two thirds of all of the freshwater inflow to the gulf (Bergström et al., 2001). As a result, the surface-layer salinity increases from about 1 in the easternmost area up to 6–7 $g kg^{-1}$ at the entrance (e.g. Haapala and Alenius, 1994). The deep layer is characterized by a slight westward salinity increase (e.g. Liblik and Lips, 2011). The seasonal thermocline forms at the beginning of May, develops during the summer and starts to erode by the end of August (e.g. Alenius et al., 1998). Thermocline is usually situated at a depth of 10–15 m and is strongest in July–August when surface layer temperature rises to an average of 17 °C in the open Gulf (Liblik and Lips, 2011). During the winter, the water masses are rather well mixed down to a depth of 60 m (Haapala and Alenius, 1994; Alenius et al., 2003). The Gulf has a free connection to the NE Baltic Proper, without a sill, and therefore salinity may increase below the halocline (located at a depth of 60–70 m, Alenius et al., 1998) in the western part of gulf up to 10 $g kg^{-1}$, i.e. the typical values of the open sea. Regarding other

OSD
10, 727–762, 2013

topographic features, greater sea depths and steeper bottom slopes are found along the southern coast (Fig. 1). The line connecting the deepest depths on cross-sections (thalweg) is located closer to the southern coast. A slight (up to 10 m) cross-gulf bottom elevation located in the sea area between Tallinn–Helsinki separates the two (western and central) deeper basins.

We have performed six surveys along the thalweg of the gulf in winter–spring 2011/2012 on board the RV Salme (Marine Systems Institute at Tallinn University of Technology): on 21 December, 24–25 January, 7–8 February, 29 February, 15–16 March and 8 May. The sampling stations were located in the western and central parts of the Gulf (Fig. 1). The westernmost station, A1, was located near the western border of the gulf, and station A10 was located some 130 km eastwards, exceeding the bottom elevation near Tallinn–Helsinki. Distance between the stations varied within a range of 10–17 km.

At all stations, vertical profiles of temperature, salinity and dissolved oxygen were recorded, using a Sea-Bird SBE 19*Plus* V2 CTD SEACAT Profiler equipped with the dissolved oxygen sensor SBE43. Dissolved oxygen profiles were not registered on 8 May; only bottom oxygen concentrations were acquired during that cruise. The quality of salinity data was checked against the water sample analyses by a high precision salinometer 8410A Portasal (Guildline). Sea-Bird SBE 19*Plus* CTD profiler overestimated salinity on average $0.041\,\mathrm{g\,kg^{-1}}$. The dissolved oxygen sensor was calibrated against water sample analyses. Altogether 60 data pairs were used to find best linear fit between dissolved oxygen (DO) values from SBE43 and from the analyses: $\mathrm{DO} = \mathrm{DO_{SBE}} \times 1.41$ ($r^2 = 0.99$), where $\mathrm{DO_{SBE}}$ is the dissolved oxygen recorded by SBE43 sensor.

2.2 Autonomous recording

We installed two buoy stations with acoustic Doppler current profilers (ADCP, 300 kHz; Teledyne RD Instruments) on the bottom of locations A3 and A9 at the depths of 91 m and 87 m, respectively. Current profilers were set to separate 40 and 38 vertical bins, respectively, by 2 m steps. The shallowest bin was at the depth range 7–9 m, and deepest at range 85–87 m and 81–83 m, respectively. A Seabird SBE 16*Plus* V2 CTD SEACAT conductivity and temperature recorder with the SBE43 dissolved oxygen sensor was also deployed at station A3. The recorder was mounted at a depth of 86 m (5 m above sea bottom). Current profilers were set to measure with a sampling interval of 30 min and SBE16 recorded data with a 1 h interval. The dissolved oxygen sensor was analogously calibrated against water sample analyses ($r^2 = 0.99$).

2.3 Wind and sea level data, NAO index

Wind data were obtained near the thalweg at Tallinnamadal Lighthouse (Fig. 1). Wind speed and direction were measured at a level of 36 m above the sea surface and reported as hourly averages. Wind speed was multiplied by a height correction coefficient of 0.91 (Launiainen and Saarinen, 1984) to reduce the recorded wind speed to the reference height of 10 m during neutral atmospheric stratification. Additionally, we used the wind data time series (1981–2012) from Kalbådagrund weather station (Finnish Meteorological Institute), since the time series at Tallinnamadal was too short for certain analyses. Wind speed and direction data from Kalbådagrund was available every third hour as a 10 min average. Keevallik and Soomere (2010) have found slight differences, both in wind direction and speed between Tallinnamadal and Kalbådagrund. In the present study we used data from the Tallinnamadal station as the main descriptor of the wind characteristics in the western Gulf during the study period. Wind velocity components were calculated along the axis from SSW to NNE, positive toward NNE. Winds from SSW are the most favorable for estuarine circulation reversal and from NNE the most favorable for estuarine circulation (Liblik and Lips, 2011).

Hourly sea level data were obtained at Kunda coastal station (Estonian Hydrological and Meteorological Institute), on the southern coast of the Gulf of Finland. Sea level values in Estonia are related to the long-term mean (0 cm).

OSD
10, 727–762, 2013

NAO index (Jones et al., 1997) data (http://www.cru.uea.ac.uk/~timo/datapages/naoi.htm) were used in order to characterize airflow during the study period and compare it with the long-term data.

2.4 Calculation procedures

Salinity values acquired from the Practical Salinity Scale (Fofonoff and Millard Jr., 1983) were multiplied by 1.0047 (Millero et al., 2008) and presented as absolute salinity ($g\,kg^{-1}$).

ADCP velocity, sea level and wind data were smoothed with a low pass filter by Butterworth (1930).

The area and volume of hypoxic near-bottom waters (oxygen concentration ≤ 90 $\mu mol\,L^{-1}$) were estimated from the O_2 profiles taken on the transect located along the thalweg, assuming that cross-transect changes are small. Using the gridded topography by Seifert et al. (2001), the observed upper boundaries of hypoxic layer were extrapolated across the transect and interpolated along the transect. The sea area used in numerical integration was limited by the western border of the Gulf of Finland and by the easternmost station, A10. The surface area of that region is approximately 10 000 km^2 and its volume is about 450 km^3. We also similarly calculated the bottom area and volume for the water with salinity ≥ 9.3 $g\,kg^{-1}$.

3 Results

3.1 Wind conditions

Prior to the start of our observation campaign on 21 December 2011, weak and moderate winds from variable directions blew during the first two decades of November (Fig. 2). From the last decade of November until the end of December, wind conditions in the study area were shaped by strong air flow from south and southwest, reaching

OSD
10, 727–762, 2013

maximum wind speed of 25 m s^{-1} on 26 December. Variable and weaker winds prevailed during the first half of January. The second half of January was shaped by a high atmospheric pressure system, resulting in low air temperatures and calm wind conditions. Southeasterly and southwesterly winds prevailed in February and southwesterly winds in March. However, prevailing winds in February–March were quite frequently interrupted by northerly winds or calm periods. Only in mid-February there was longer continuous period with southeasterly and southwesterly winds. As is typical of spring, variable and weaker winds were observed from April until the end of the study period.

3.2 CTD and O_2 transects along the thalweg

A weakly stratified water column was observed on 21 December (Fig. 3). The density difference between near-bottom and surface water did not exceed 0.7 kg m^{-3} along the thalweg. At stations A2–A7 the density difference was 0.3 kg m^{-3} or smaller. Salinity in the whole section was relatively low: It was over 7.0 g kg^{-1} only in the near-bottom layer at the westernmost station, A1, and at stations A8–A10. The along-gulf surface layer salinity gradient was relatively weak, and salinity changed from 6.2–6.3 g kg^{-1} in the easternmost part to 6.4–6.5 g kg^{-1} in the westernmost part. Temperature was clearly over the maximum density temperature in the whole section and varied in the range 5.8–7.1 °C. The water column in the whole section was well oxygenated, and even at near-bottom depths oxygen concentration at all stations was over 220 µmol L^{-1} (5 mL L^{-1}).

On 24–25 January a well-defined deep salt water wedge was observed at stations A1–A6, separated from the upper mixed layer by a strong halocline. Salinity above the halocline varied in the range of 6.4–6.8 g kg^{-1}, while in the deep layer values up to 9.9 g kg^{-1} were observed. The halocline was relatively sharp, for instance a salinity increase from 6.8 to 9.8 g kg^{-1} was observed in the depth range of 75–76.5 m at station A4. Vertical salinity distribution at easterly stations (A7–A10) was clearly more uniform. Temperature varied in a range of 3.1–6.0 °C, increasing with depth and decreasing

OSD
10, 727–762, 2013

eastward. Oxygen conditions in the section were strongly related to the extent of the salt wedge. The water column above the salt wedge was well oxygenated: oxygen concentrations were > 360 µmol L^{-1} (8 mL L^{-1}). As a result of salt water intrusion, the bottom was covered by hypoxic water at stations A1–A6 while at stations A7–A10 water was well oxygenated. Furthermore, near-bottom oxygen conditions were even improved at the easternmost stations, compared to the previous survey.

Two weeks later, by 7–8 February, the deep layer salt wedge was observed some 15 km eastward from its former position. The slight increase of salinity was also observed at the three easternmost stations. The development of a near-surface halocline was observed in the upper part of the water column at a 10–20 m depth at all stations. The surface layer water temperature varied in a range from –0.2 to 0.8 °C and its salinity was in the range of 4.7–5.5 g kg^{-1} at stations A3–A10, while at the two westernmost stations temperature and salinity were 0.8–0.9 °C and 6.0 g kg^{-1}, respectively. Near-bottom layer oxygen content was slightly declined along the whole section, but in the eastern part of the study area oxygen concentrations were still over 270 µmol L^{-1} (6 mL L^{-1}) in the entire water column.

On 29 February the section was not fully completed due to heavy ice conditions. Available data from the western part of the section showed westward movement of a deep layer salt wedge. The halocline was still detectable at the westernmost station, A1, where salinity was over 9 g kg^{-1}. The density difference between bottom and surface water was at all recorded stations over 1 kg m^{-3}. Similarly to the deeper layer, the near-surface halocline had weakened and in some stations was absent in the upper part of the water column. Surface layer salinity was still characterized by a strong decrease toward the east, from 6.8 g kg^{-1} (A1) to 5.2 g kg^{-1} (A7). The surface layer temperature was below 0 °C at stations A4–A7 while it was slightly over 0 °C at the westernmost stations, A1–A3. With the exception of the near-bottom layer at station A1, oxygen was at all stations above 90 µmol L^{-1}.

By 15–16 March the reformation of both haloclines had occurred. The salt water wedge in the deep layer as well the fresher water in the upper layer was evident at all stations. The eastward decrease of surface salinity was from 5.8 (A1) to 5.0 $g\,kg^{-1}$ (A10) in the upper layer and from 10.2 to 8.4 $g\,kg^{-1}$ in the near bottom layer, respectively. Temperature distribution was characterized by an increase from 0 °C to 5.5 °C from the surface to the near-bottom layer. The re-appeared hypoxic salt wedge affected deep water oxygen content over the whole section. However, at the easternmost stations, A8–A10, water in the bottom layer still contained oxygen over 90 $\mu mol\,L^{-1}$. Compared to the situation on 7–8 February, the hypoxic water layer above the bottom was thicker. In the western half of the section, oxygen concentration decreased below 90 $\mu mol\,L^{-1}$ already at 71–74 m depth.

The last survey along the thalweg was conducted at the end of the study period on 8 May. The upper layer temperature has increased to 4–5 °C. The cold intermediate layer was between 20 and 50 m depth. In comparison to the previous survey the salinity in the upper 35 m layer showed minor changes. The upper layer halocline resided at the 25 m depth. Deep saline water had extended over the entire section, so that deep water halocline was observed between 65 and 75 m depth. The isohaline of 7 $g\,kg^{-1}$ had been lifted up from 50–60 m to 40–50 m depth between the two surveys, which indicates eastward transport of the lower layer water. The density difference between surface and bottom layer was at least 3 $kg\,m^{-3}$ at all stations. Oxygen distribution was consistent with deep water salinity distribution showing that near-bottom water was hypoxic at all stations. Nevertheless, a slight increase in oxygen along the gulf from 4–9 $\mu mol\,L^{-1}$ (0.1–0.2 $mL\,L^{-1}$) at the three westernmost stations to 54–71 $\mu mol\,L^{-1}$ (1.2–1.6 $mL\,L^{-1}$) at the three easternmost stations was still evident.

3.3 Time series of current profiles, temperature, salinity and oxygen

At both of the two measurement sites the currents were variable and occasionally very strong (Figs. 4 and 5). Average current speeds in the eastern part of study area (A9) were from 7.5 $cm\,s^{-1}$ at 82 m depth (deepest measured bin) to 11.6 $cm\,s^{-1}$ at 8 m depth (shallowest measured bin) while the maximum recorded speeds were in the range of

40–56 cm s^{-1} in the upper 30 m and 33–40 cm s^{-1} below that depth. At station A3 the flow was on average stronger in the deep layer and in the upper layer (11–13 cm s^{-1}), and slightly weaker in intermediate layer (9–11 cm s^{-1}). The highest recorded current speeds were in the range of 35–49 cm s^{-1} at 26–86 m depth while it was over 52 cm s^{-1} in the upper part (8–26 m) of the water column. The strongest current of 88 cm s^{-1} was recorded during a southwesterly storm event on 26 December at a depth of 12 m.

The temporal course of cumulative wind stress showed that reversal-favorable winds started on 25 November and lasted until 5 January (Fig. 6). The cumulative wind stress was approximately 11 N m^{-2} d^{-1} for that period. At the onset of winds the sea level at Kunda rose from −10 cm up to 66 cm (36 h low pass filtered). The last 18 days of flow reversal (21 December–8 January) were covered by measurements. Vertical flow structures at both measurement sites were dominated by barotropic outflow, opposite to the wind direction, from the last decade of December until the first half of January (Figs. 4 and 5), i.e. during the period of weak haline stratification (Fig. 3b). In the reversal period beginning on 21 December, temperature, salinity and dissolved oxygen concentration varied in a relatively narrow range: 5.0–6.6 °C, 6.5–6.8 g kg^{-1} and 326–380 µmol L^{-1} (7.3–8.5 mL L^{-1}), respectively. A temperature decrease throughout the period was evident, though, and also shorter period fluctuations with simultaneous changes in salinity were observed: an increase of 0.5 °C in temperature was accompanied by a salinity increase of about 0.1 g kg^{-1}.

Since 8 January short-term wind turnings from south to northeast were well reflected in the deep layer current, where previously prevailing outflow was temporary replaced by inflow. This period of variable flow regime ended on 14 January with the help of 1.5 days of northerly wind impulse and a following period of weaker winds (Fig. 2). The re-establishment of estuarine circulation caused a deep salt wedge intrusion to the location of station A3 (Fig. 3e) and interrupted barotrophic flow (Fig. 4); however, the haline stratification and current shear at the location of station A9 (Fig. 5) still remained quite weak. Inflow prevailed in the whole water column until mid-February, and was particularly strong in the deep layer. The re-establishment of estuarine circulation coincided well with the decline of the sea level in the gulf. In the near-bottom layer, dissolved oxygen levels during the estuarine circulation period almost never exceeded 45 µmol L^{-1} (1 mL L^{-1}), while salinity varied in a range of 9.4–10.3 g kg^{-1} (Fig. 6). Contrary to the earlier period, increases in salinity were accompanied with slight decreases in temperature.

The second reversal event was induced by southerly winds beginning in mid-February and peaking after southerly winds prevailed for 12 days; cumulative wind stress for that period was 2 N m^{-2} d^{-1}. Reversal-favorable winds raised the sea level and altered the estuarine flow in the deep layer. Strong outflow in the deep layer that actually extended to a 30–40 m depth with simultaneous inflow in the upper layer was observed in the second half of February at westerly station A3 (Fig. 4). The event was also recognizable at easterly station A9 (Fig. 5) where inflow prevailed in the upper 20 m and outflow over the rest of the water column. Compared to the strong near-bottom outflow at location A3, the outflow was at a maximum in the middle of the water column and was much weaker at location A9. The second reversal event was not as strong as the one observed in December–January. The reversal event peaked at a dissolved oxygen concentration of 210 µmol L^{-1} (4.7 mL L^{-1}), while salinity decreased to 8.2 g kg^{-1} simultaneously. Dissolved oxygen concentration and salinity fluctuated in a relatively wide range during the event and correlated strongly.

As a consequence of a short wind impulse from the north at the beginning of March, inflow re-appeared in the deep layer, the sea level declined and the salt wedge was re-established simultaneously at the buoy station on 3 March. The flow structure at location A3 was multi-layered with the strongest current shear in the deep halocline, but the mean flow was to the east over the entire water column. Although we observed short periods with outflow in the deep layer and simultaneous slight decreases/increases in salinity and oxygen, respectively; oxygen concentration remained below 45 µmol L^{-1} (1 mL L^{-1}) until the end of the study period on 8 May. At the same time that flow was weaker, but more persistent, at station A9, outflow prevailed in the upper layer and

OSD
10, 727–762, 2013

inflow in the deep layer, which on average resulted in typical estuarine flow in the eastern part of study area.

3.4 Effects of reversal events on oxygen conditions in the gulf

A hypoxic near-bottom salt wedge, originating from the NE Baltic Proper, penetrated to the gulf in the middle of January, after a reversal event lasting since the end of November. The salt wedge had reached station A6 by 24–25 January and a similar situation was also observed on 7–8 February. On 29 February, during a weaker reversal event, hypoxic water was present only at the westernmost station. It re-appeared at station A3 on 3 March. By 15–16 March, the salty and hypoxic water re-appeared along the thalweg at stations A1–A7 while at the three easternmost stations near-bottom oxygen concentration was still over 90 µmol L^{-1}. The thickness of the hypoxic water column increased, as compared to the situation during previous cruises. On 8 May hypoxic water was present at all stations, but oxygen values in the eastern part were still slightly higher than in the western part of the study area.

Oxygen concentrations within and below the halocline were strongly related to the salinity. Estimated sea areas and volumes occupied by hypoxic water and by water with salinity ≥ 9.3 g kg^{-1} were strongly correlated ($n = 5$; $r^2 = 0.99$, $r^2 = 0.98$, respectively; $p < 0.01$). The hypoxic bottom areas and volumes of hypoxic water during estuarine circulation and during reversal events demonstrate well how drastic changes in bottom oxygen conditions could occur in winter without remarkable biological activity (Table 1). The estimated bottom area covered by hypoxic water was > 1300 km^2 on 15–16 March while it was almost hypoxic-free even during the relatively weak reversal event in February–March. The hypoxic area and volume were even greater after the spring bloom on 8 May.

OSD
10, 727–762, 2013

4 Discussion

Along-thalweg mapping and time-series observations at the near-bottom layer revealed high variability in the thermohaline structure and oxygen concentration of the Gulf of Finland. We found that vertical flow structure, especially the bottom current, is the most important driver shaping the deep water characteristics in winter: oxygen conditions in the bottom layer of the gulf can be explained by spatio-temporal variability of the salt wedge. We observed two estuarine circulation reversal events with durations of 1.5 and 0.5 months, in December–January and February–March, respectively. As a consequence, stratification was greatly weakened, current structure altered and the hypoxic salt wedge disappeared during those events. Elken et al. (2003) demonstrated on the basis of vertical temperature-salinity profiles from one repeated station that rapid weakening of the halocline cannot be explained by vertical mixing. Our results, which show that near-bottom water characteristics were associated with lateral water exchange, are well in accordance with their findings.

Halocline disappearance and re-appearance events occurred simultaneously with strong near-bottom currents. The re-establishment of a deep layer salt wedge might occur very rapidly, within 12 h. Estuarine circulation re-activations were associated with a strong inflow and reversal event in February started with strong outflow in the deep layer. However, when reversal weakened stratification drastically, as in December–January, then upwind barotropic flow along the thalweg was observed and current shear maximum disappeared together with the halocline. The current structure in the deep layer of the gulf is not rigorously studied, but strong near-bottom currents seem to be a quite common feature of the gulf (Almroth et al., 2009; Lagemaa et al., 2010; Liblik and Lips, 2012). Strong wind-induced currents in the deep layer have been observed also in other estuaries, such as in Long Island Sound (Whitney and Codiga, 2010). The observed upwind barotropic flow along the thalweg allows us to assume a temporary wind-induced two-cell circulation in the Gulf: a well-developed reversal event resulted in downwind barotropic flow along the shores and upwind barotropic compensation flow along the thalweg, as is typical in semi-enclosed homogeneous basins (e.g. Sanay and Valle-Levinson, 2005). Further investigations are needed to answer that question.

Shifts in flow regime in the deep layer were quite dependent on wind forcing. We found the best correlation ($r^2 = 0.44$, $p < 0.01$, $n = 3323$) between low-pass filtered (36 h) NNE wind and along-gulf axis inflowing current in the deep layer, when a time lag of 18 h was taken into account. It is a slightly longer lag compared to Elken et al. (2003) who applied a 15 h offset in the model experiment. Cumulative wind stress of about 1 $\mathrm{N\,m^{-2}\,d^{-1}}$ was required to start the second reversal event but weak wind (–0.2 $\mathrm{N\,m^{-2}\,d^{-1}}$) preceded both estuarine circulation re-activation events. Once estuarine circulation was established, it maintained well by gravitational forcing without supporting wind forcing, e.g. the period between two reversal events from mid-January to mid-February (see Fig. 6). Moreover, estuarine circulation withstands the reversal of favorable winds to some extent. Elken et al. (2003) found that estuarine circulation may be altered, if the southwesterly wind component exceeds the mean value by at least 4–5.5 $\mathrm{m\,s^{-1}}$.

The strength of stratification depended mainly on the presence of the halocline in the deep layer due to the salt wedge intrusion, and on the presence of a near-surface halocline in the upper layer due to relatively fresher water in the surface layer. The simultaneous appearance of salty water in the deep layer and fresher riverine water in the surface layer has been observed in across the gulf section in summer (Lips et al., 2009). However, in summer the effect of this phenomenon on stratification is not as drastic (Liblik and Lips, 2012), since the water column is also thermally stratified. Wind-driven impact on estuarine circulation and respective changes in stratification were also observed in Liverpool Bay (Simpson et al., 1990), in Chesapeake Bay (Scully et al., 2005; Li and Li, 2011) and in the Rio de la Plata estuary (Meccia et al., 2013). In our study, during the reversal events the density difference between near-bottom and surface water declined below 0.3 $\mathrm{kg\,m^{-3}}$, while it exceeded 3 $\mathrm{kg\,m^{-3}}$ during the estuarine circulation prevailing period. Thus, a well-developed reversal event could result in complete mixing of the water column. The reversal event probably peaked and complete mixing occurred between the two cruises on 22 December and 24–25 January. The water column was completely mixed and homogenous at the two easternmost stations even on 24–25 January while the salt wedge was already present at the rest of the stations. To our knowledge, with the exception of the sill-separated Gulf of Bothnia (Håkansson et al., 1996), such a complete mixing event has never been observed in deep basins of the Baltic Sea.

Considering wind statistics and analysis of routine CTD measurements in the Gulf of Finland, wintertime reversal events occur quite often and the frequency of occurrence shows increasing tendency since the 1990s (Elken et al., 2012). However, the approximately 1.5-month-long reversal event observed in December–January was rather uncommon. In order to evaluate the probability of such a reversal event, we briefly analyzed the NAO index data since 1822 and Kalbådagrund wind data since 1981 for autumn–winter. The NAO index of 3.20 in December 2011 clearly exceeded the long-term mean of 0.31 for December. The monthly NAO index in December has been higher than 3.20 only seven times since 1822, most recently in December 1986. The monthly NAO index ≥ 3.20 in January and February have been more common, with 15 and 25 cases registered since 1822, respectively. The mean monthly NAO index of 1.72 in September–November 2011 was clearly higher than the long-term mean of –0.31. Only in five years since 1822 has the mean NAO index been higher than 1.72, indicating that airflow from the southwest was exceptionally intensive in autumn 2011. The strong relationship between NAO and oxygen conditions has been detected also in the eastern part of the gulf (Eremina et al., 2012). Collected temperature and salinity profiles in the study area (A1 and A6, unpublished data) suggested that haline stratification was weakened already in September–October. Monthly averages of the wind component from SSW to NNE in Kalbådagrund in November 2011 and January–April 2012 were close to long-term means (1981–2012) and varied in a range from $-0.3\,\mathrm{m\,s^{-1}}$ to $2.2\,\mathrm{m\,s^{-1}}$. However, December 2011 was extraordinary, and the monthly mean wind component was $7.6\,\mathrm{m\,s^{-1}}$, which is far greater than the long-term mean of $2.0\,\mathrm{m\,s^{-1}}$ for that month and pointed to the clear dominance of a SSW wind. Until December 2011

OSD
10, 727–762, 2013

the highest monthly mean SSW wind speed favorable for reversal since 1981 has been 6.2 $m\,s^{-1}$ in November 1982 and 1986.

Oxygen content and salinity were strongly related, which was revealed most prominently in coinciding halocline and oxycline. Longitudinal excursions of the salt wedge defined the strength of vertical stratification and near bottom oxygen content locally (Fig. 7). During the first reversal event the stratification was weak and near bottom water was well oxygenated (366 $\mu mol\,L^{-1}$ or 8.2 $mL\,L^{-1}$ on average) in the deep layer in the western part of the study area. The same tendency was observed in the case of the relatively weak reversal event observed in February. During periods of estuarine circulation the stratification increased and oxygen concentration was clearly under 90 $\mu mol\,L^{-1}$. The estimated bottom area covered by hypoxic water was > 1300 km^2, and the volume of this water was approximately 12 km^3 in mid-March (Table 1, Fig. 8). Near-bottom oxygen concentrations were even lower and estimated hypoxic area and volume were greater on 8 May. With respect to the cross-gulf inclination of the halocline (Lips et al., 2009), our hypoxic area estimations are rather slightly underestimated than overestimated, given the fact that the thalweg of the gulf (our study section) is closer to the southern coast. Intensification of estuarine circulation often causes improvement in oxygen conditions (e.g. Tokyo Bay, Sato et al., 2012). In that respect, the Gulf of Finland is a rather unique marine system, since here intensification of estuarine circulation leads to an increase of hypoxic water area and volume. A similar estuarine system is found in the Lower St. Lawrence estuary, where bottom water, isolated by permanent halocline from the upper layer, has to travel several years before it arrives at the estuary (Gilbert at al., 2005).

Reversal events had longer-lasting effects on oxygen conditions in the deep layer in the eastern part of the study area (Fig. 7). On 15–16 March, two months after the re-appearance of the hypoxic salt wedge in the western part of the gulf, the three easternmost stations in the study area were still hypoxic-free. Elken et al. (2012) have shown that stratification collapse events quite frequently occur in the central part of the gulf in winter. Our results indicate that relatively weak stratification and well-oxygenated

OSD
10, 727–762, 2013

water in the central part of the gulf could occur simultaneously with a hypoxic salt wedge in the deep layer in the western part of the gulf (Fig. 7). That could be related to the topography of the gulf – a slight (up to 10 m) bottom elevation located in the sea area around station A7 (Fig. 1). This slightly shallower section of the thalweg impeded the salt wedge from spreading to the east. However, if the thickness of the salt wedge was sufficient, as on 8 May, it penetrated further to the east and occupied the bottom layer of the thalweg entirely. Furthermore, eastward advection of the salt wedge can lead to hypoxic conditions even in the eastern part of the Gulf (the Russian waters of the Gulf between Kotlin and Hogland islands) (Eremina et al., 2012).

The saline and hypoxic water origin in the NE Baltic Proper is based on the considerations of topography and mean stratification. During the 24–25 January cruise we additionally acquired CTD profiles at two stations in the northern Baltic Proper: Estonian National Monitoring Station 25 at a sea depth of 100 m, and the international, 170 m-deep monitoring station H2 (Fig. 8). The hypoxic salt water wedge at station 25 was approximately 20 m thick and situated at a depth range from 80 m to the bottom. The hypoxic water there seemed to be a mixture of two waters: saltier and slightly colder water, originating from H2 at a depth range of 110–115 m, and warmer water from the upper part of halocline. The hypoxic deep layer found at westernmost station A1 was a mixture of salty near-bottom water from station 25, and relatively fresher and warmer water. The origin of this fresher and warmer water seemed to be also outside the Gulf of Finland, since the water column temperature was below 6 °C for that time in the gulf. Thus, the deep water salt wedge, observed in the study area on 24–25 January after a major reversal event, originated from the northern Baltic Proper at a depth range of 110–115 m. This is probably deeper than normal due to seasonal weakening and decline of the halocline in the northern Baltic Proper (Matthäus, 1984). Secondly, Elken et al. (2006) showed that counter-estuarine transport in the Gulf of Finland reduces the vertical stability and decreases the halocline in the NE Baltic Proper.

Current structure in the deep layer during development of the second reversal event (Fig. 4) indicated that weakening of the halocline and oxygenation of bottom water was probably related to the horizontal advection. For confirmation we plotted salinity-oxygen diagrams and profiles before the reversal event (7–8 February) and during the reversal event (29 February) at station A3 (Fig. 9). It can be seen from consecutive salinity and oxygen profiles that saltier and hypoxic water disappeared from the deep layer at the A3 station by 29 February, while in the layer above (10–70 m) an increase of salinity and decrease of oxygen was not detected. Thus, pure vertical mixing could not produce this disappearance event. This fresher and oxygenated bottom water originated from the eastern part of the thalweg – the deep layer water at station A3 on 29 February had a similar oxygen content and salinity as the deep layer water observed at the A7 station on 7–8 February (see oxygen-salinity plot on Fig. 9). An opposite change in salinity occurred simultaneously in the upper 10 m layer, but there was probably also some vertical mixing involved, as the 10–30 m layer had become fresher. Similar changes in upper layer salinity were observed in summer during the dominance of southwesterly winds (Liblik and Lips, 2012). Therefore, halocline disappearance and oxygenation of bottom water could be related to the advection of oxygen-rich water from the eastern part of the study area. However, when eastward transport of relatively saltier water in the upper layer and westward transport of relatively fresher water in the deep layer lasts long enough, it can cause complete mixing of the water column. The homogenous water column observed at the two easternmost stations on 24–25 January was probably the consequence of such an event.

Oxygen-depletion related effects have clear impacts on biogeochemical cycles in the Baltic Sea (HELCOM, 2009). Simultaneously with the expedition on 24–25 January, the Estonian national monitoring survey was conducted and near-bottom water samples collected for nutrient analysis near the thalweg. Nutrient concentrations clearly differed in hypoxic and in well-oxygenated deep layer waters. NH_4, NO_2+NO_3 and PO_4 concentrations in water affected by the hypoxic salt wedge were in the range of 4.2–6.4, 0.1–2.3 and 2.7–4.0 $\mu mol\,L^{-1}$, respectively, while in well-oxygenated near-bottom water concentrations were in the range of 0.1–0.2, 6.8–8.1 and 0.9–1.0 $\mu mol\,L^{-1}$, respectively. This confirms earlier findings, according to which hypoxic conditions in the near-bottom layer cause phosphorus release from sediment (e.g. Viktorsson et al., 2012) and interruption of the nitrification-denitrification chain along with ammonium enrichment (e.g. Jäntti et al., 2012) in the Gulf of Finland. In that respect, reversal events affect the nutrient pool of the Gulf of Finland in three ways: (1) interrupting estuarine transport of phosphate-rich waters from the Baltic Proper (Lips et al., 2008), (2) allowing more efficient diapycnal mixing (Elken et al., 2003) and nutrient transport to the euphotic zone due to weaker stratification (Reissmann et al., 2009), and (3) altering benthic nutrient dynamics in the Gulf (Hietanen et al., 2007). Thus, reversal events potentially have an effect on the whole ecosystem of the Gulf.

5 Conclusions

The wintertime temporary reversals of standard estuarine circulation obviously influence stratification and oxygen conditions in the Gulf of Finland. As a consequence of two circulation reversals observed in winter 2011/2012, stratification was greatly weakened, current structure altered and the hypoxic salt wedge disappeared during those events. The well-developed reversal event (December–January) lasted about 1.5 months and caused the complete vanishing of stratification, barotropic flow along the thalweg and almost homogenous oxygen concentrations in the whole water column. Shifts from estuarine circulation to reversed circulation and vice versa were both associated with strong currents (up to 40 $cm\,s^{-1}$) in the deep layer. Vertical stratification and oxygen conditions in the deep layer were defined by longitudinal to and fro migrations of the salt wedge. The hypoxic salt wedge originated from the NE Baltic Proper at a depth range of 110–115 m. Thus, deterioration of deep layer oxygen conditions was solely related to the advective transport of hypoxic water from the NE Baltic Proper. Likewise, weakening of the halocline and oxygenation of near-bottom water was most likely related to westward advection along the thalweg. However, long-lasting counter-advective transports in the upper and deep layer resulted in convection and complete mixing of the whole water column.

OSD
10, 727–762, 2013

Change from oxygenated to hypoxic conditions at the entrance to the gulf occurred very rapidly, within 12 h.

The near-bottom layer of the gulf was almost hypoxic-free even in instances of relatively weak reversal during February–March. However, during estuarine circulation periods the estimated bottom area covered by hypoxic water was > 1300 km^2. Reversal events had longer-lasting effects on near-bottom oxygen conditions in the eastern part of the study area, where hypoxic-free conditions remained two months after the re-appearance of the hypoxic salt wedge in the western part of the Gulf. That could probably be related to the topography of the Gulf – the shallower sea area between Tallinn–Helsinki on the thalweg may have prevented the salt wedge from spreading to the east. However, if estuarine circulation had prevailed long enough, it could have penetrated further to the east and occupied the bottom layer of the thalweg entirely.

Acknowledgements. This study was supported by the Estonian Science Foundation (grant Nos. 9278 and 9382) and the EstKliima project, funded by Environmental Protection and Technology Programme No. 3.2.0802.11-0043 of the European Regional Fund. The Finnish Meteorological Institute kindly provided Kalbådagrund wind data, and the Estonian Meteorological and Hydrological Institute the sea level data. We are thankful to Tarmo Kõuts for providing Tallinnamadal wind data and Sergei Stjopin for providing nutrient data. Likewise, we thank the crew of RV Salme and our colleagues at the Marine Systems Institute for performing field measurements.

References

Alenius, P., Myrberg, K., and Nekrasov, A.: The physical oceanography of the Gulf of Finland: a review, Boreal Env. Res., 3, 97–125, 1998.

Alenius, P., Nekrasov, A., and Myrberg, K.: Variability of the baroclinic Rossby radius in the Gulf of Finland, Cont. Shelf Res., 23, 563–573, 2003.

Almroth, E., Tengberg, A., Andersson, J. H., Pakhomova, S., and Hall, P. O. J.: Effects of resuspension on benthic fluxes of oxygen, nutrients, dissolved inorganic carbon, iron and manganese in the Gulf of Finland, Baltic Sea. Cont. Shelf Res., 29, 807–818, 2009.

Bergström S. and Carlsson, B.: River runoff to the Baltic Sea: 1950–1990, Ambio, 23, 280–287, 1994.
Butterworth, S.: On the theory of filter amplifiers, Experimental Wireless and the Wireless Engineer, 7, 536–541, 1930.
Conley, D. J., Humborg, C., Rahm, L., Savchuk, O. P., and Wulff, F.: Hypoxia in the Baltic Sea and basin-scale changes in phosphorus biogeochemistry, Environ. Sci. Technol., 36, 5315–5320, 2002.
Conley, D. J., Björck, S., Bonsdorff, E., Carstensen, J., Destouni, G., Gustafsson, B. G., Hietanen, S. Kortekaas, M., Kuosa, H., Meier, H. E. M., Müller-Karulis, B., Nordberg, K., Norkko, A., Nürnberg, G., Pitkänen, H., Rabalais, N. N., Rosenberg, R., Savchuk, O. P., Slomp, C. P., Voss, M., Wulff, F. and Zillén, L.: Hypoxia-related processes in the Baltic Sea, Environ. Sci. Technol., 43, 3412–3420, 2009.
Diaz, R. J. and Rosenberg, R.: Spreading dead zones and consequences for marine ecosystems, Science, 321, 926–929, doi:10.1126/science.1156401, 2008.
Elken, J., Raudsepp, U., and Lips, U.: On the estuarine transport reversal in deep layers of the Gulf of Finland, J. Sea Res., 49, 267–274, 2003.
Elken, J., Mälkki, P., Alenius, P., and Stipa, T.: Large halocline variations in the Northern Baltic Proper and associated meso- and basin-scale processes, Oceanologia, 48, 91–117, 2006.
Elken, J., Raudsepp, U., Laanemets, J., Passenko, J., Maljutenko, I., Pärn, O., and Keevallik, S.: Increased frequency of wintertime stratification collapse events in the Gulf of Finland since the 1990s, J. Marine Syst., in review, 2012.
Eremina, T. R., Maximov, A. A., and Voloshchuk, E. V.: The influence of climate's variability on the deep-water oxygen conditions in the east of the Gulf of Finland, Oceanology, 52, 771–779, 2012.
Fofonoff, N. P. and Millard Jr., R. C.: Algorithms for computation of fundamental properties of seawater, Unesco Tech. Pap. Mar. Sci., 44, 1–58, 1983.
Fonselius, S. and Valderrama, J.: One hundred years of hydrographic measurements in the Baltic Sea, J. Sea Res., 49, 229–241, 2003.
Gilbert, D., Sundby, B., Gobeil, C., Mucci, A., and Tremblay, G. H.: A seventy-two-year record of diminishing deep-water oxygen in the St. Lawrence estuary: the northwest Atlantic connection, Limnol. Oceanogr., 50, 1654–166, 2005.
Haapala, J. and Alenius, P.: Temperature and salinity statistics for the northern Baltic Sea 1961–1990, Finnish Mar. Res., 262, 51–121, 1994.

OSD
10, 727–762, 2013

Håkansson B., Alenius, P., and Brydsten, L.: Physical environment in the Gulf of Bothnia, Ambio Spec. Rep. 8, 5–12, 1996.
Hansen, D. V. and Rattray, M.: New dimensions in estuary classification, Limnol. Oceanogr., 11, 319–326, 1966.
HELCOM (Helsinki Commission): Eutrophication in the Baltic Sea: an integrated thematic assessment of the effects of nutrient enrichment in the Baltic Sea region, Baltic Sea Environment Proceedings, 115, 1–20, 2009.
Hietanen, S. and Lukkari, K.: Effects of short-term anoxia on benthic denitrification, nutrient fluxes and phosphorus forms in coastal Baltic sediment, Aquat. Microb. Ecol., 49, 293–302, doi:10.3354/ame01146, 2007.
Jäntti, H. and Hietanen, H.: The effects of hypoxia on sediment nitrogen cycling in the Baltic Sea, Ambio, 41, 161–169, doi:10.1007/s13280-011-0233-6, 2012.
Jones, P. D., Jonsson, T., and Wheeler, D.: Extension to the North Atlantic Oscillation using early instrumental pressure observations from Gibraltar and South-West Iceland, Int. J. Climatol., 17, 1433–1450, 1997.
Keevallik, S. and Soomere, T.: Towards quantifying variations in wind parameters across the Gulf of Finland, Est. J. Earth Sci., 59, 288–297, 2010.
Kullenberg, G.: Physical oceanography, in: The Baltic Sea, Elsevier Publishing Company, Amsterdam, 135–182, 1981.
Lagemaa, P., Suhhova, I., Nõmm, M., Pavelson, J., and Elken, J.: Comparison of current simulations by the state-of-the-art operational models in the Gulf of Finland, in: IEEE Conference Proceedings, IEEE/OES Baltic 2010 International Symposium, 25–27 August 2010, Riga, Latvia, 1–11, 2010.
Laine, A. O., Andersin, A.-B., Leiniö, S., and Zuur, A. F.: Stratification-induced hypoxia as a structuring factor of macrozoobenthos in the open Gulf of Finland (Baltic Sea), J. Sea Res., 57, 65–77, 2007.
Launiainen, J. and Saarinen, J.: Marine wind characteristics in the northern Baltic Sea, Finnish, Mar. Res., 250, 52–86, 1984.
Li, Y. and Li, M.: Effects of wind on stratification and circulation in a partially mixed estuary. J. Geophys. Res., 116, C12012, doi:10.1029/2010JC006893, 2011.
Liblik, T. and Lips, U.: Characteristics and variability of the vertical thermohaline structure in the Gulf of Finland in summer, Boreal Env. Res. A, 16, 73–83, 2011.

OSD
10, 727–762, 2013

Liblik, T. and Lips, U.: Variability of synoptic-scale quasi-stationary thermohaline stratification patterns in the Gulf of Finland in summer 2009, Ocean Sci., 8, 603–614, doi:10.5194/os-8-603-2012, 2012.
Lips, U., Lips, I., Liblik, T., and Elken, J.: Estuarine transport versus vertical movement and mixing of water masses in the Gulf of Finland (Baltic Sea), in: IEEE Conference Proceedings, US/EU-Baltic Symposium "Ocean Observations, Ecosystem-Based Management & Forecasting", Tallinn, 27–29 May 2008, IEEE, 2008, (IEEE Conference Proceedings), 1–8, 2008.
Lips, I., Lips, U., and Liblik, T.: Consequences of coastal upwelling events on physical and chemical patterns in the central Gulf of Finland (Baltic Sea), Cont. Shelf Res., 29, 1836–1847, 2009.
MacCready, P. and Geyer., W. R.: Advances in estuarine physics, Ann. Rev. Mar. Sci., 2, 35–58, 2010.
Matthäus, W.: Climatic and seasonal variability of oceanological parameters in the Baltic Sea, Beitr. Meereskd., 51, 29–49, 1984.
Matthäus, W. and Lass, H. U.: The recent salt inflow into the Baltic Sea, J. Phys. Oceanogr., 25, 280–286, 1995.
Meccia, V. L., Simionato, C. G., and Guerrero, R. A.: The Rio de la Plata estuary response to wind variability in synoptic timescale: salinity fields and salt wedge structure, J. Coast. Res., 29, 61–77, 2013.
Millero, F. J., Feistel, R., Wright, D. G., and McDougall, J.: The composition of standard seawater and the definition of the reference-composition salinity scale, Deep-Sea Res. Pt. I, 55, 50–72, doi:10.1016/j.dsr.2007.10.001, 2008.
Reissmann, J. H., Burchard, H., Feistel, R., Hagen, E., Lass, H. U., Mohrholz, V., Nausch, G., Umlauf, L., and Wieczorek, G.: Vertical mixing in the Baltic Sea and consequences for eutrophication – a review, Prog. Oceanogr., 82, 47–80, 2009.
Sanay, R. and Valle-Levinson, A.: Wind-induced circulation in semienclosed homogeneous, rotating basins, J. Phys. Oceanogr., 35, 2520–2531, 2005.
Sato, C., Nakayama, K., and Furukawa, K.: Contributions of wind and river effects on DO concentration in Tokyo Bay, Estuar. Coast. Shelf S., 109, 91–97, 2012.
Savchuk, O. P.: Large-scale dynamics of hypoxia in the Baltic Sea, in: Chemical Structure of Pelagic Redox Interfaces: Observation and Modelling, Hdb. Env. Chem., 22, Springer Verlag, Berlin, Heidelberg, Germany, 137–160, 2010.

OSD
10, 727–762, 2013

Scully, M. E., Friedrichs, C., and Brubaker, J.: Control of estuarine stratification and mixing by wind-induced straining of the estuarine density field, Estuaries, 28, 321–326, 2005.
Seifert, T., Tauber, F., and Kayser, B.: A high resolution spherical grid topography of the Baltic Sea – 2nd edition, Baltic Sea Science Congress, Stockholm 25–29 November 2001, Poster #147, available at: www.io-warnemuende.de/iowtopo, 2001.
Simpson, J. H., Brown, J., Matthews, J., and Allen, G.: Tidal straining, density currents, and stirring in the control of estuarine stratification, Estuaries, 13, 125–132, 1990.
Vahtera, E., Conley, D. J., Gustafsson, B. G., Kuosa, H., Pitkänen, H., Savchuk, O. P., Tamminen, T., Viitasalo, M., Voss, M., Wasmund, N., and Wulf, F.: Internal ecosystem feedbacks enhance nitrogen-fixing cyanobacteria blooms and complicate management in the Baltic Sea, Ambio, 36, 186–194, 2007.
Viktorsson, L., Almroth-Rosell, E., Tengberg, A., Vankevich, R., Neelov, I., Isaev, R., Kravtsov, V., and Hall, P. O. J.: Benthic Phosphorus Dynamics in the Gulf of Finland, Aquat. Geochem., 18, 543–564, doi:10.1007/s10498-011-9155-y, 2012.
Whitney, M. M. and Codiga, D.: Response of a large stratified estuary to wind events: observations, simulations, and theory for Long Island Sound. J. Phys. Oceanogr., 41, 1308–1327, 2011.
Zillén, L., Conley, D. J., Andrén, T., Andrén, E., and Björck, S.: Past occurrences of hypoxia in the Baltic Sea and the role of climate variability, environmental change and human impact, Earth-Sci. Rev., 91, 77–92, 2008.

OSD
10, 727–762, 2013

Estuarine circulation reversals and related changes in oxygen

T. Liblik et al.

Table 1. Estimated hypoxic bottom areas and hypoxic water volumes. 8 May values were calculated on the basis of bottom oxygen concentrations and salinity profiles: Linear regression between sea areas and volumes occupied by hypoxic water and by water with salinity $\geq 9.3\,\mathrm{g\,kg^{-1}}$ was used in estimation.

Cruise/area/volume	Hypoxic area (km^2)	Hypoxic water volume (km^3)
21 December	0	0
24–25 January	510	2.6
7–8 February	770	4.9
29 February	130	0.8
15–16 March	1380	12.0
8 May	1650	14.6

OSD
10, 727–762, 2013

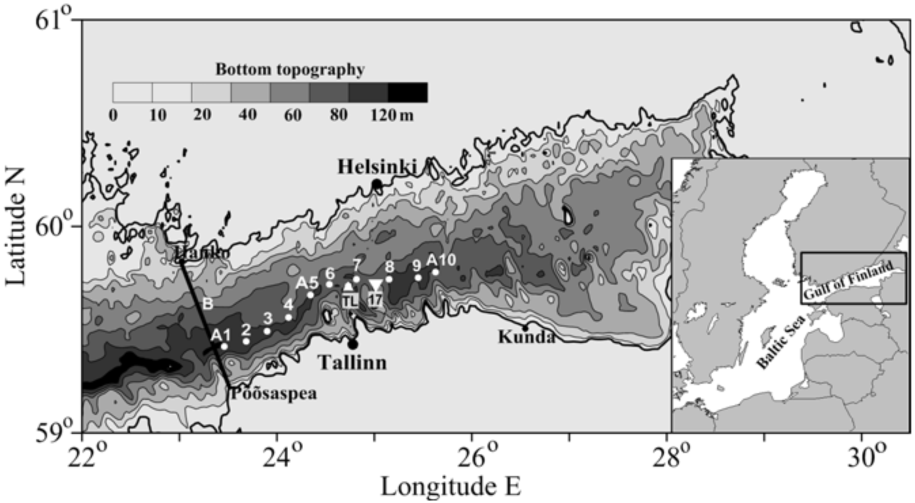

Fig. 1. Map of the study area in the Gulf of Finland. The solid white circles represent the locations of the CTD stations (A1–A10) along the thalweg of the gulf. The two bottom-mounted ADCP were located at CTD stations A3 and A9. The bottom-mounted ADCP at location A3 was equipped with a CTD and dissolved oxygen sensor. The solid white square represents the location of the wind measurements at Tallinnamadal Lighthouse (TL). The solid white triangle (17) represents the Estonian national monitoring station. The bottom topography is drawn from the gridded topography in meters (Seifert et al., 2001). The western border of the gulf is defined as the line from Põõsaspea–Hanko town (line B).

OSD
10, 727–762, 2013

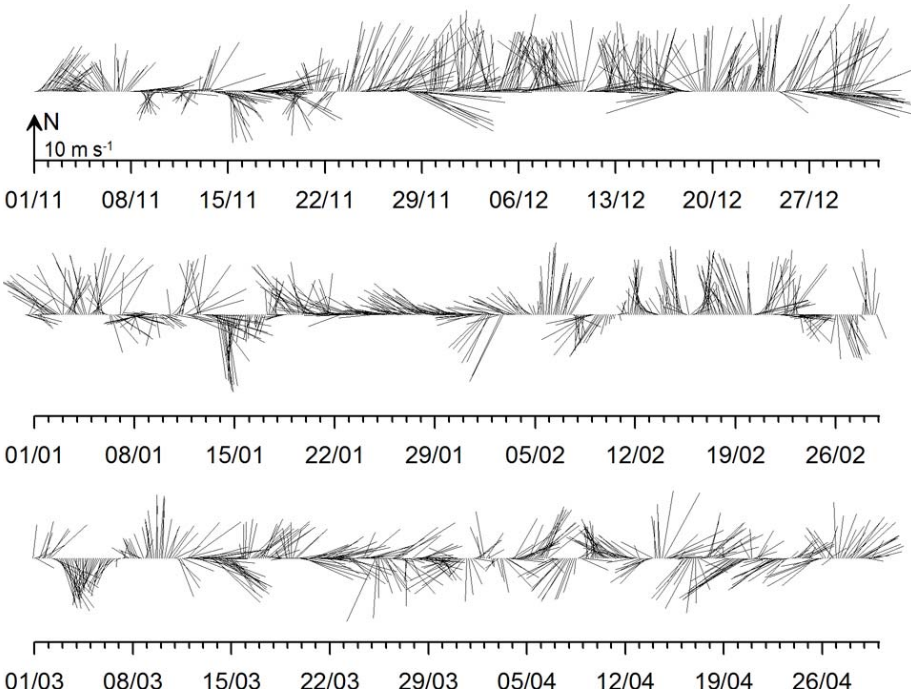

Fig. 2. Time series of the 10 m level Tallinnamadal wind vector from 1 November 2011 to 30 April 2012.

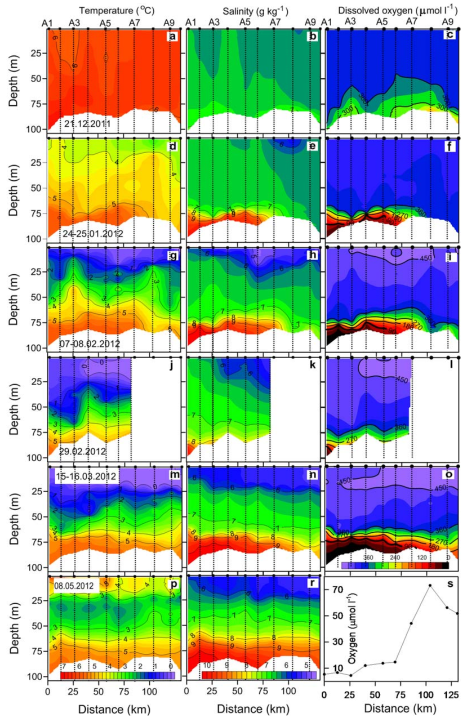

Fig. 3. Vertical sections of temperature (interval 0.25 °C), salinity (interval 0.25 g kg^{-1}) and dissolved oxygen (interval 30 µmol L^{-1}) on 21 December 2011 **(a,b,c)**, 24–25 January 2012 **(d, e, f)**, 7–8 February **(g, h, i)**, 29 February **(j, k, l)**, 15–16 March **(m, n, o)** and 8 May **(p, r)** measured along the thalweg of the Gulf. Bold contour marks the dissolved oxygen concentration of 90 µmol L^{-1}. On 8 May only near-bottom layer dissolved oxygen concentrations were available **(s)**. Values on the x-axis indicate distance from the westernmost station (see Fig. 1).

OSD
10, 727–762, 2013

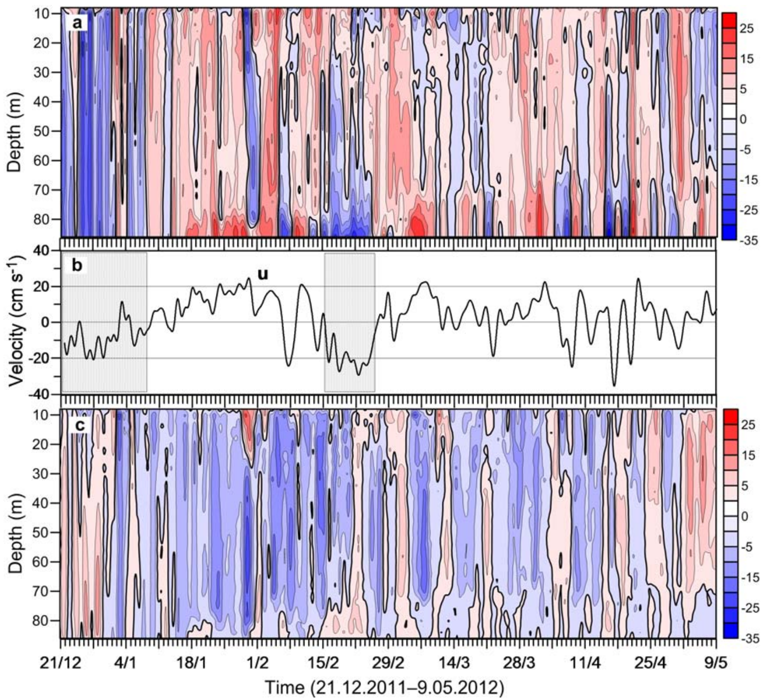

Fig. 4. (a) Temporal course of vertical distribution of low-pass filtered along-gulf axis current velocity component (u) and **(c)** cross-gulf axis current velocity component (v) in cm s^{-1} at the location of mooring station A3 from 21 December 2011 to 9 May 2012. Positive velocities (red) display the inflow into the gulf or northward flow, and negative velocities (blue) display opposite, respectively. **(b)** Temporal course of along-gulf axis current velocity component (u) at the depth of 85 m. Shaded areas mark time intervals when developed estuarine circulation reversals were observed at location A3.

OSD
10, 727–762, 2013

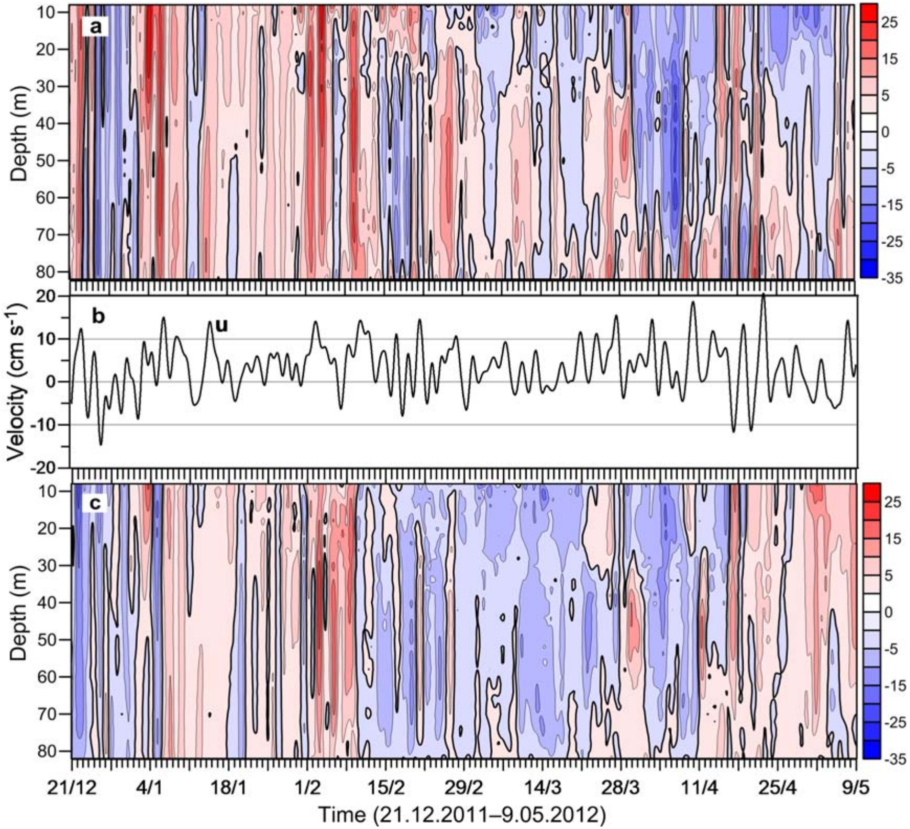

Fig. 5. (a) Temporal course of the vertical distribution of low-pass filtered along-gulf axis current velocity component (*u*) and **(c)** cross-gulf axis current velocity component (*v*) in cm s^{-1} at the location of mooring station A9 from 21 December 2011 to 9 May 2012. Positive velocities (red) display the inflow into the gulf or northward flow, and negative velocities (blue) display opposite, respectively. **(b)** Temporal course of along-gulf axis current velocity component (*u*) at a depth of 85 m.

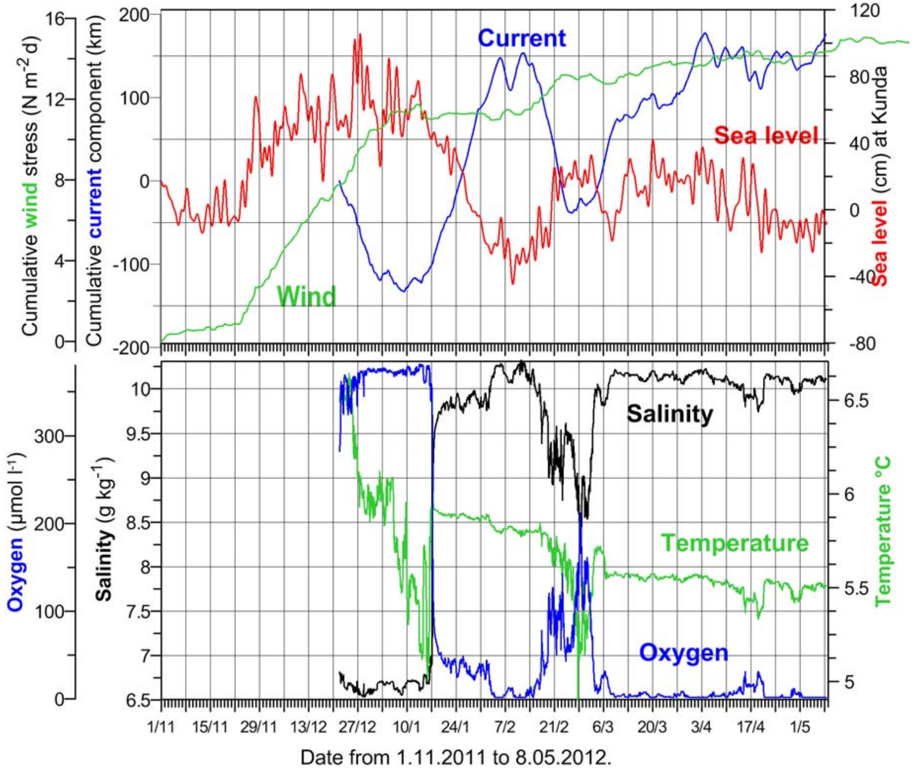

Fig. 6. Cumulative along-gulf axis current velocity component (km, blue line), cumulative wind stress ($N\,m^{-2}d$, green line) and low-pass filtered sea level (cm) time series in the upper panel. Hourly time series of salinity ($g\,kg^{-1}$, black line), temperature (°C, green line) and dissolved oxygen ($\mu mol\,L^{-1}$, blue line) in the lower panel. Temperature, salinity, dissolved oxygen and current were measured at location A3 from 21 December 2011 to 8 May 2012 at the depth of 85 m (at a height of about 5 m from bottom). Wind and sea level measurements were obtained at Tallinnamadal Lighthouse and Kunda coastal station, respectively.

OSD
10, 727–762, 2013

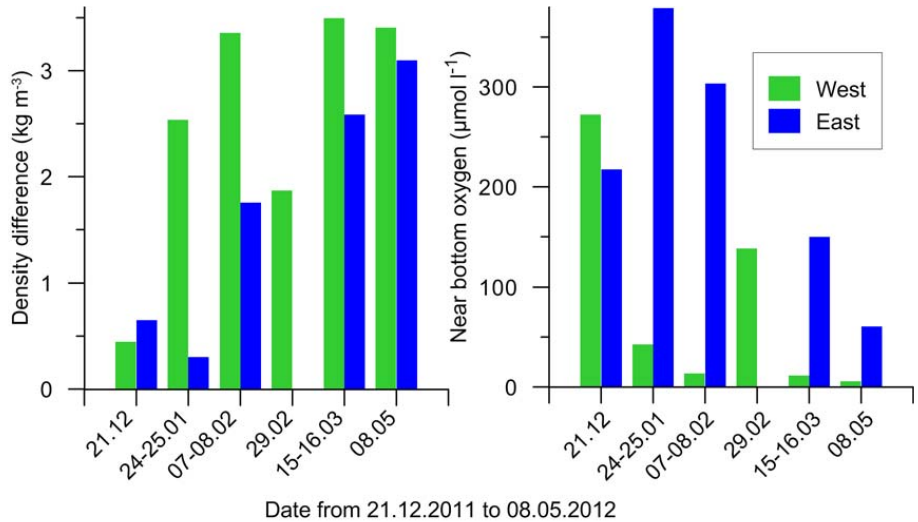

Fig. 7. Average density difference between near-bottom and surface water (kg m^{-3}, left panel) and oxygen concentration in the near-bottom layer (µmol L^{-1}, right panel) at westernmost stations A1–A3 (green) and easternmost stations A8–A10 (blue) from 21 December to 8 May. On 29 February only the western part of the section was visited.

OSD
10, 727–762, 2013

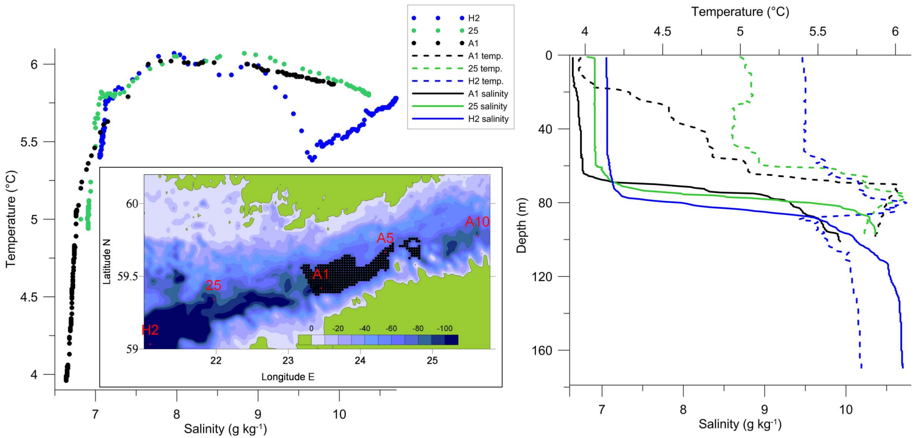

Fig. 8. TS-diagrams (dots on left panel), temperature (°C, dashed lines on right panel) and salinity profiles ($g\,kg^{-1}$, solid lines on right panel) on 24–25 January; and hypoxic area (black area on left panel) on 15–16 March. TS-diagrams and profiles at station H2 (blue), 25 (green) and A1 (black). Hypoxic area was estimated only between the western border of the Gulf of Finland and the easternmost station A10 (Fig. 1). The bottom topography is drawn from the gridded topography in meters (Seifert et al., 2001).

OSD
10, 727–762, 2013

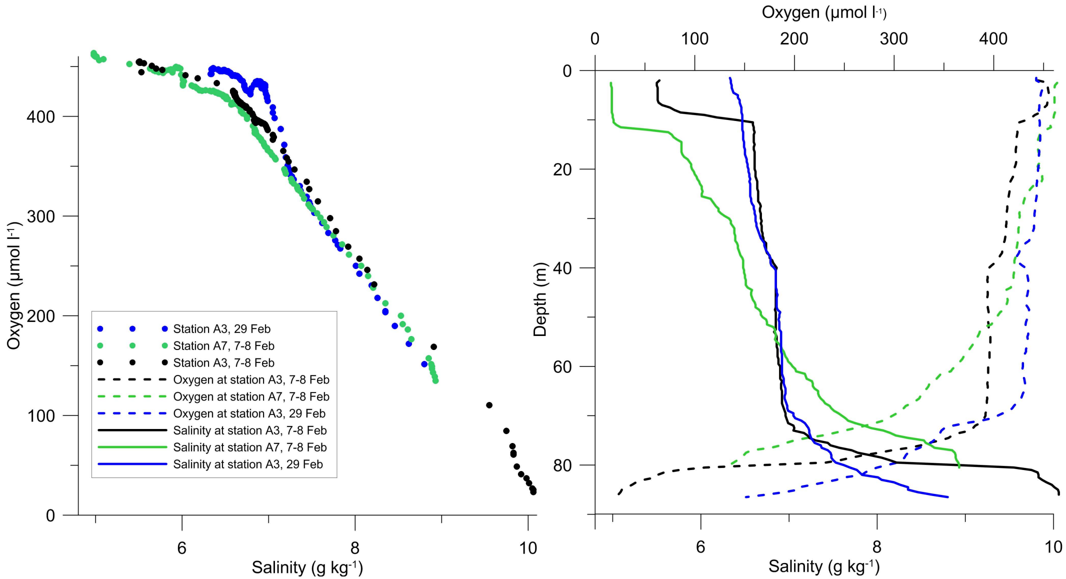

Fig. 9. Oxygen-salinity diagrams (dots on left panel), and salinity ($\mathrm{g\,kg^{-1}}$, solid lines on right panel) and dissolved oxygen ($\mathrm{\mu mol\,L^{-1}}$, dashed lines on right panel) profiles on 7–8 February (black) and on 29 February (blue) at station A3, and on 7–8 February (green) at station A7.